

激光熔覆原位自生 TiC—VC 颗粒增强 Fe 基金属陶瓷涂层

杜宝帅, 李清明, 王新洪, 邹增大

(山东大学 材料科学与工程学院, 济南 250061)

摘 要: 采用钛铁、钒铁、石墨等组分, 利用 5 kW 横流 CO₂ 激光器, 氩气保护在低碳钢板上制备了致密、无孔隙与基体呈冶金结合的原位自生 TiC—VC 复合碳化物颗粒增强 Fe 基熔覆层。利用金相显微镜、X 射线衍射、电子探针及显微硬度计, 研究了熔覆层的显微组织及性能。结果表明, 钛铁、钒铁与石墨通过激光熔覆的反应, 所得细小的 TiC—VC 复合碳化物增强相弥散分布 Fe 基体之中, 熔覆层硬度从基体到表面呈梯度分布, 较基体有显著提高。

关键词: 激光熔覆; 原位自生; TiC—VC 颗粒

中图分类号: TG159.9 **文献标识码:** A **文章编号:** 0253-360X(2007)04-065-04



杜宝帅

0 序 言

激光熔覆技术以其熔池具有快速凝固、涂层与基体呈冶金结合、稀释率低等特点, 在耐磨、抗蚀、热障等涂层制备方面显示出良好的应用前景^[1-3]。陶瓷颗粒增强金属基复合材料综合了陶瓷相的高强度、高硬度和金属基体良好的韧性, 是一种性能优良的耐磨涂层, 在工程构件的表面修复及强化领域已获得了成功应用。利用激光熔覆技术制备金属陶瓷涂层具有很好的发展前景, 已引起了有关研究人员的关注^[4-6]。目前为止, 其制备方式主要有两种外加颗粒法和颗粒原位自生法。外加颗粒法虽然工艺简便, 易于获得所需陶瓷相, 但陶瓷颗粒在熔覆过程中易烧损, 而且颗粒因污染而易导致与基体结合性差, 颗粒相尺寸及分布状态也难于控制。原位自生金属陶瓷涂层由于增强相通过反应原位生成, 增强颗粒弥散分布, 无界面污染且同基体结合良好, 因而涂层具有较高的硬度及良好的耐磨性。

TiC 颗粒具有高硬度、高弹性模量, 而且热力学性能稳定, 是一种理想的陶瓷增强相, 国内外研究人员已经利用激光熔覆技术成功制备出 TiC 增强 Ni 基及 Fe 基涂层^[7,8]。但其制备方式一般为通过钛粉与石墨直接反应形成, 纯钛粉成本较高, 而且 Ti 元

素性质活泼, 易与在熔覆过程中氧化烧损。V 也为强碳化物形成元素, 它与碳的反应产物 VC 具有与 TiC 相近的性质, 而且它对钢基体具有更好的润湿性。文献[9]在 FeCrSiB 合金粉末中直接添加纯钛、钒粉, 原位反应制备了 TiC—VC 增强 Fe 基涂层。其研究结果表明 Ti 与 V 的复合添加可促进增强相的形成, 对获得原位生成颗粒增强复合涂层具有非常显著的效果。

利用激光熔覆技术, 以廉价钛铁、钒铁、石墨为原料, 通过它们之间的冶金反应形成 TiC—VC 复合碳化物粒子, 不仅可以克服添加单质元素易氧化烧损的缺点, 而且易于促进碳化物颗粒的形成。作者采用该方法制备 TiC—VC 增强 Fe 基金属陶瓷涂层, 并对其显微组织和性能进行了研究。

1 试验材料及方法

基体材料采用 Q235 钢, 试样尺寸为 50 mm×20 mm×6 mm, 试样表面在熔覆前经打磨并用丙酮清洗。合金粉末由工业用钛铁、钒铁粉(其化学成分见表 1), 铁粉(99% 纯度, 200 目), 石墨(纯度 99.5%)按一定比例混合组成, 为了改善涂层组织性能还加入了少量稀土元素。熔覆前合金粉末采用水玻璃作粘结剂预置在试板表面, 厚度约为 1.5 mm。试板晾干后经 2 h 60 °C 烘干。激光器为 5 kW 横流 CO₂ 激光器, 熔覆用功率为 3 kW, 扫描速度 5 mm/s,

光斑直径3 mm。为防止涂层熔覆过程氧化,采用氩气进行保护,氩气流量为20 L/min。

表 1 钛铁钒铁化学成分(质量分数, %)

Table 1 Chemical composition of ferrotitanium and ferrovanadium

牌号	Ti	V	Al	Si	C	Fe
FeTi25	25~25.5	—	<8	<3	<0.1	余量
FeV45	—	45~45.5	<1.5	<3	<1.0	余量

沿横截面制备金相试样,经研磨抛光后用王水化学腐蚀。利用 DMax — Rc 型 X 射线衍射仪 (CuK α),对熔覆层的相结构进行分析,利用 JXA — 8800R 型电子探针针对熔覆层成分进行微观分析,利用 Shimadzi 显微硬度计对熔覆层的显微硬度进行了测量。

2 试验结果及讨论

2.1 显微组织及物相分析

图1为涂层表面 X 射线衍射结果。由图可见,熔覆层主要由 α -Fe、TiC、VC 和 Fe₃C 组成。证明了钛铁、钒铁及石墨经激光熔覆,制备出原位生成 TiC、VC 增强的 Fe 基熔覆层。

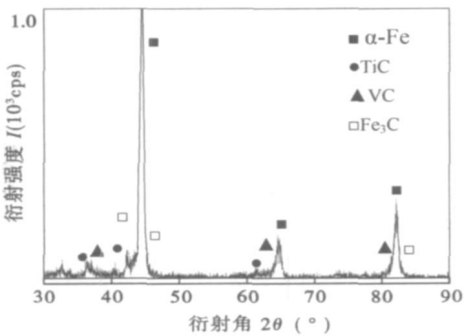


图 1 熔覆层 X 射线衍射结果
Fig. 1 XRD spectra of cladding layer

图2为试样横截面的显微组织形貌。由图 2a 可以看出试样分为三个区域:熔覆区、过渡区和热影响区。熔覆层组织致密,未见裂纹和气孔产生。由图可以看出熔覆层与基体形成了良好的冶金结合,由于结合界面处温度梯度和凝固速度比值很大,凝固组织以低速平界面生长,因而形成了白亮带。图 2b 为熔覆层内部组织,可看出白色碳化物颗粒均匀分布在基体上。

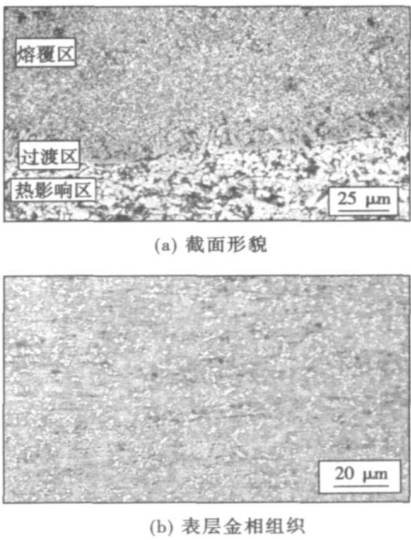


图 2 熔覆层金相组织
Fig. 2 Optical micrographs of clad coating

图 3a 为采用 JXA — 8800 型电子探针针对熔覆层所作的二次电子像,可见细小的块状、树枝状碳化物粒子弥散分布于基体之中。图 3b 为对点 A 以及基体

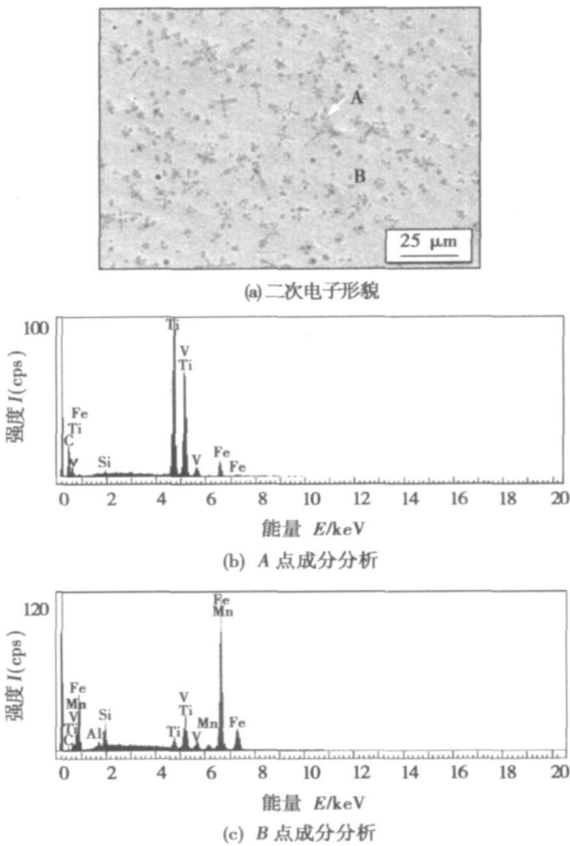


图 3 熔覆层二次电子形貌及 EDS 点成分分析
Fig. 3 Secondary electron imaging and EDS spot analysis of clad coating

组织所做的点成分分析, 结果表明 A 点成分为: C 52.10%, Ti 26.75%, V 15.82%, Si 0.43%, Fe 4.90% (摩尔分数)。由结果可知块状化合物的主要成分为 Ti 和 V, 证明碳化物为 TiC-VC 的复合体。在熔池凝固过程中, 快速迁移的固液界面将反应生成的 TiC-VC 颗粒捕获, 从而使颗粒弥散分布于基体之中, 大量的复合碳化物增强相的形成可显著提高熔覆层硬度, 提高其耐磨性。

2.2 原位反应生成 TiC 和 VC 热力学分析

熔覆层材料在激光的作用下熔化形成熔池, 处于 Fe-Ti-V-C 反应体系之中。在此反应体系之中可能存在多个反应。FeTi 和 FeV 在高温熔池中发生熔化分解, 从而导致 Ti 和 V 溶解于液相 Fe 之中。Ti 和 V 为强碳化物形成元素, 在熔池中可以存在以下反应 $Ti + C = TiC$, $V + C = VC$ 。图 4 表明了各种反应产物的 Gibbs 生成自由能。从图中可以看出 TiC 和 VC 的 Gibbs 生成自由能均为负值, 而且相对于其它产物热力学性质更为稳定, 因而从热力学角度分析通过钛铁、钒铁与石墨之间的反应可以合成 TiC-VC 增强粒子。

图 5 为各元素面分布图, 可以看出块状化合物富 Ti, V, C 元素, 贫 Fe, 判断为 TiC, VC 复合碳化物

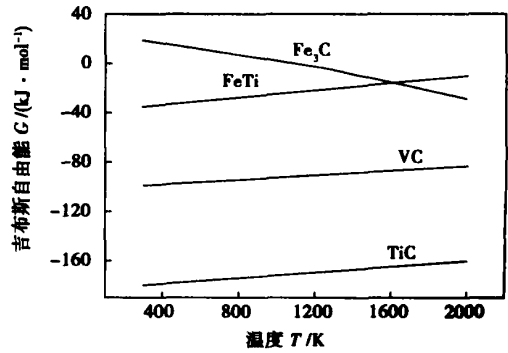


图 4 Fe-Ti-V-C 体系各化合物吉布斯生成自由能
Fig. 4 Gibbs free energy of reaction in Fe-Ti-V-C system

颗粒。TiC 和 VC 均为面心立方结构, 且其晶格常数接近, 具有良好的相容性, 细小的 TiC, VC 颗粒在熔池凝固过程中极易相互结合依附生长, 形成 TiC-VC 互溶体的复合碳化物结构。从图中可以看出 V 元素的分布更为弥散, 证明基体中固溶了较多 V 元素。另外, 相对 TiC, VC 对 Fe 基体具有更小的润湿角, 因而在熔池快速凝固过程中更易被凝固界面所捕获, 从而使微细的 VC 粒子弥散分布于基体之中。

图 6 为激光熔覆层的截面硬度分布曲线, 由于

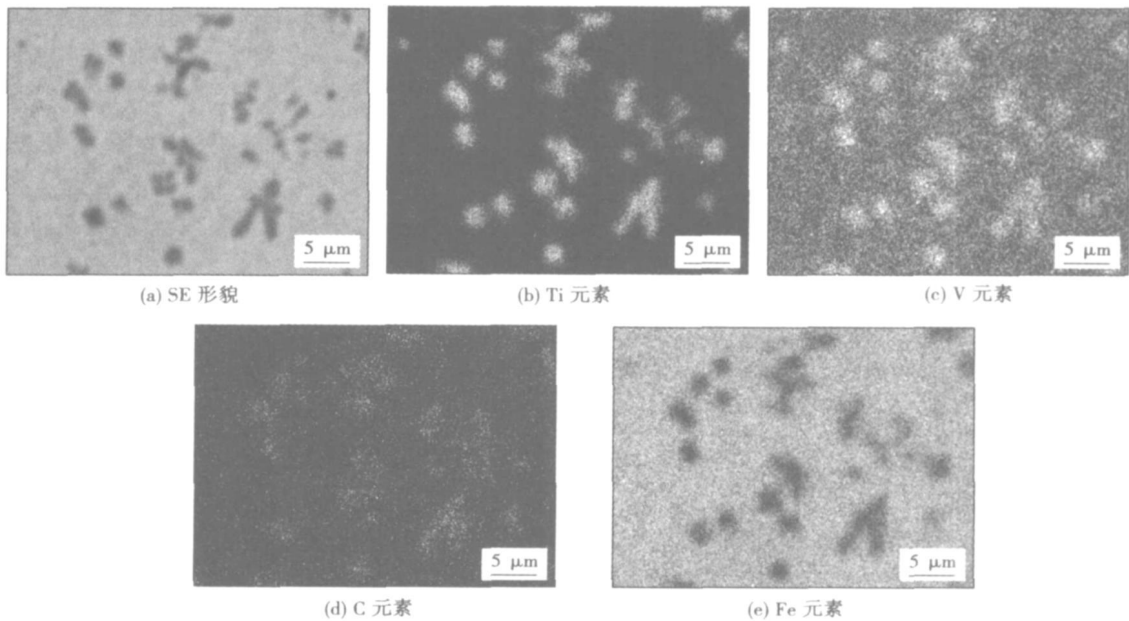


图 5 熔覆层各元素面分布图
Fig. 5 EPMA face scanning of elements in clad coating

激光熔覆过程中形成的熔池内部存在强烈的流体对流, 密度较小的 TiC-VC 复合碳化物颗粒容易上浮, 从而导致熔覆层中碳化物呈梯度分布^[10], 熔覆

层上部碳化物含量较高, 因而硬度较高。总体上由于 TiC-VC 增强相的存在, 熔覆层硬度相对基体显著提高。

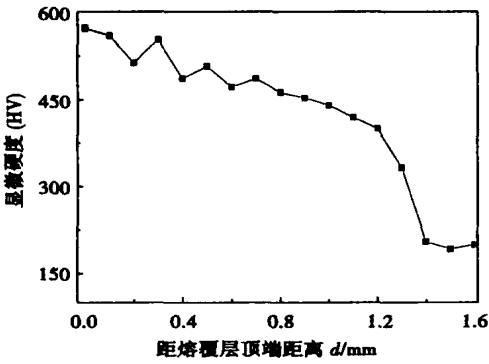


图 6 激光熔覆层的硬度分布图

Fig. 6 Microhardness distribution of clad coating

3 结 论

(1) 采用激光熔覆技术,通过钛铁、钒铁同石墨之间的冶金反应,制备了原位自生 TiC - VC 复合碳化物粒子增强 Fe 基涂层,所得涂层同基体呈良好冶金结合,无缺陷。增强相弥散均匀分布于基体之中。

(2) 电子探针元素面分析结果表明,熔覆层中增强粒子为 TiC - VC 互溶体构成的复合碳化物。弥散分布的增强相可显著提高熔覆层显微硬度。

参考文献:

[1] Riabkina Fishman M, Rabkin E, Levin P, *et al.* Laser produced

functionally graded tungsten carbide coatings on M2 high-speed tool steel[J] . Materials Science and Engineering A, 2001, 302(1): 106—114.

[2] Chen Y, Wang H M. Eutectic MC carbide growth morphologies of a laser clad TiC /FeAl composite coating[J] . Materials Letters, 2005, 59(28): 3699—3702.

[3] 高 阳, 潘 峰, 佟百运, 等. 铜基材上热障涂层的激光熔覆[J] . 中国有色金属学报, 2003, 13(2): 315—318.

[4] Sen Yang, Na Chen, Wenjin, *et al.* Fabrication of nickel composite coatings reinforced with TiC particles by laser cladding[J] . Surface and Coatings Technology, 2004, 183(2—3): 254—260.

[5] Meng Q W, Geng B L, Zhang Y. Laser cladding of Ni-base composite coatings onto Ti—6Al—4V substrates with pre-placed B4C+NiCrBSi powders[J] . Surface and Coatings Technology, 2006, 200(16—17): 4923—4928.

[6] 田永生, 陈传忠, 王德云, 等. 激光熔覆生成碳硅钛化合物及其组织性能研究[J] . 中国激光, 2004, 31(7): 880—882.

[7] 武晓雷, 陈光南. 激光形成原位 TiC 颗粒增强涂层的组织及性能[J] . 金属学报, 1998, 34(12): 1284—1288.

[8] Man H C, Zhang S, Cheng F T. Microstructure and formation mechanism of in situ synthesized TiC /Ti surface MMC on Ti—6Al—4V by laser cladding[J] . Scripta Materialia, 2001, 44(12): 2801—2807.

[9] 张锦英, 马明星, 刘文今. 钒、钛对激光熔覆铁基原位生成颗粒增强复合涂层组织的影响[J] . 金属热处理, 2003, 28(8): 1—4.

[10] Pei Y T, Zou T C. Gradient microstructure in laser clad TiC—reinforced Ni-alloy composite coating[J] . Materials Science and Engineering A, 1998, 241(1—2): 259—263.

作者简介: 杜宝帅, 男, 1982 年出生, 博士研究生。主要从事激光表面强化技术的研究, 发表论文 2 篇。

Email: dubaoshuai@gmail.com

grated. Non-instruct topology information of product-department-joint was described in the model. Structure of model and consistence of operation were analyzed. An example data of product structure tree was showed. Integration method of graphic data between CAD and welding computer aided process planing (WCAPP) based on litmus-less meta file was analyzed. The solution of process document based on multi-type template mechanism was offered, which ensure the criterion of data operation and outputting of process document.

Key words: welding computer aided process planing; extended Marked language; welding process; process card

Self-optimizing control for laser cutting quality based on coaxial vision

ZHANG Yongqiang^{1,2}, CHEN Wuzhu¹, ZHANG Xudong¹, SHAN Jiguo¹ (1. Department of Mechanical Engineering, Tsinghua University, Beijing 100084, China; 2. Shougang Technical Research Institute, Beijing 100041, China). p58—60

Abstract: A sensing and control system, which includes coaxial vision sensor, DSP processor and open NC system, was designed for CO₂ laser cutting. By coaxially detecting the images of the sparks jet, it is found that the maximal sparks length of the coaxial image, which can be determined by the highest pixels of different brightness ranges of the sparks image, corresponds to the best roughness of cutting face. Experiments for self-optimizing control of laser cutting quality were performed by utilizing the images of sparks jet. The results show that the optimal cutting speed for the best roughness of the bottom edge could be found automatically and quickly.

Key words: laser cutting; quality monitoring; visual vision; self-optimizing control

Laser sintering experiment of Fe—C mixed powder

FAN Chunhua, DONG Lihua, WANG Dongsheng (Engineering Training Center, Shanghai Maritime University, Shanghai 200135, China). p61—64

Abstract: The Fe—C mixed powder without low melting-point adhesive was sintered by selective laser sintering machine, and the effect of sintering parameters on sintering formation was studied. The relationship between sintering thickness with laser power, scan interval and scanning velocity were analyzed. The relation formula between scan interval and sintering thickness was established and was verified with experiment. The sintering mechanism and balling-phenomena were studied through microstructure. The complex metal part with comparative accuracy and density was obtained under reasonable sintering parameters.

Key words: laser sintering; metal powder; process parameters

In situ synthesis of TiC-VC particles reinforced Fe-based metal matrix composite coating by laser cladding

DU Baoshuai, LI Qingming, WANG Xinhong, ZOU Zengda (School of Materials Sci-

ence and Engineering, Shandong University, Jinan 250061, China). p65—68

Abstract: Using a 5 kW CO₂ laser, in situ synthesized TiC-VC particles reinforced Fe-based alloy composite coating was prepared by preplaced ferrotitanium, ferrovanadium and graphite etc. The microstructure and properties of the composite coatings were investigated by optical microscope, X-ray diffractometer, electron probe microanalyzer and microhardness tester. Results indicated that TiC-VC particles are produced by direct metallurgical reaction among ferrotitanium, ferrovanadium and graphite during laser cladding process. It was also found that fine TiC-VC particles are dispersed in the matrix. The microhardness of the coatings, which was enhanced by the TiC-VC particles, was much greater than that of the Q235 substrate.

Key words: laser cladding; in situ synthesis; TiC—VC particles

Analysis for toughness of 2205 duplex stainless steel pipe welds

LI Weiwei, LIU Yinglai, XIONG Qingren, JI Linggang (The Key Laboratory for Mechanical and Environmental Behavior of Tubular Goods, CNPC, Xi'an, 710065, China). p69—72

Abstract: 2205 duplex stainless steel possesses favorable mechanical properties and good corrosion resistance, and is applied widely in transport, oil and natural gas, ocean and chemistry industry, etc. Compared to general austenitic stainless steel, duplex stainless steel is its difficult to weld. One natural gas the maximum operation pressure in one collection pipe of natural gas transport is 13.3 MPa and still generally considered as material which are minimum operation temperature is -30°C, and very high toughness was required for the pipe welds. The Charpy impact toughness and fracture toughness (CTOD) of longitudinal welds (used SAW methods) and girth welds (used GTAW+ SMAW methods) of 2205 duplex stainless steel pipe used for high pressure nature gas transport were tested and analyzed. The results show that the impact toughness and fracture toughness of longitudinal welds is better than that of the girth weld markedly. The main reason of these results is concern with difference of filler metal and microstructure phase ratio caused by difference heat input and postweld heat treatment.

Key words: duplex stainless steel; pipe; weld; toughness

Factors influenced arc-excited ultrasonic intensity

HU Xing, HAO Hongwei, WEN Xiongwei, HE Longbiao, LI Luming, WU Minsheng (Department of Mechanical Engineering, Tsinghua University, Beijing 100084, China). p73—76

Abstract: To enhance the understanding and control of arc-excited ultrasonic, factors that influence the arc-excited ultrasonic intensity were studied. Firstly, a welding information acquisition system was built to track the signal variations during the welding process, and it was effective to record the signal. Secondly, the varia-